Published in : Polymer Chemistry (2025), vol. 16, n°26, pp. 3041–3050
DOI: 10.1039/D5PY00384A
Status : Postprint (Author's version)

POLY(Ε-L-LYSINE)-DECORATED PARTICLES WITH TUNABLE MORPHOLOGY BY COMBINATION OF UGI MULTICOMPONENT POLYMERISATION AND RAFT- MEDIATED PISA

Thi Phuong Thu Nguyen,[a] Lei Lei,[a] Emily G. Dixon,[b] Clémence Le Coeur,[a][c] Vincenzo Taresco,[b] Antoine Debuigne[d] and Benoit Couturaud[a]*

[a] *Université Paris Est Créteil, Institut de Chimie et Matériaux Paris-Est, UMR 7182 2-8 rue H. Dunant, F-94320, Thiais, France.*
[b] *School of Chemistry, University Park, Nottingham NG7 2RD, United Kingdom.*
[c] *Laboratoire Léon Brillouin, CEA-CNRS (UMR-12), CEA Saclay, Université Paris- Saclay, 91191, Gif-sur-Yvette Cedex, France*
[d] *Center for Education and Research on Macromolecules (CERM), University of Liege (ULiege), Quartier Agora, 13 Allée du Six Août, Sart-Tilman, B-4000 Liège, Belgium.*

We report herein the unprecedented combination of Ugi multicomponent reaction (Ugi MCR) and Polymerisation-Induced Self-Assembly (PISA) to fabricate poly(ε-L-Lysine) (PεLL) decorated amphiphilic nanoparticles. First, by one-pot Ugi MCR of Boc-protected L-lysine with addition of a trithiocarbonate (TTC) compound, a macromolecular chain transfer agent (macroCTA) for Reversible Addition-Fragmentation chain-Transfer (RAFT) polymerisation was synthesised. The obtained PεLL-TTC is then used for chain extension of the hydrophobic 2-hydroxypropyl methacrylate (HPMA) in water. The reaction proceeds via the PISA mechanism, leading to the formation of amphiphilic block copolymers that self-assemble into a variety of morphologies— including spheres, short worm-like structures, and vesicles— spanning sizes from below 100 nm to over 1 µm. This work showcases a proof-of-concept to prepare water-dispersed nanoparticles decorated with polypeptoids which are highly desired in biological applications (e.g. stealth-cargo in nanomedicine, bio-separation, antibacterial coating, etc.).

Published in : Polymer Chemistry (2025), vol. 16, n°26, pp. 3041–3050
DOI: 10.1039/D5PY00384A
Status : Postprint (Author's version)

Introduction

Polymerisation-Induced Self-Assembly (PISA) has emerged as a powerful technique for generating self-assembled nanoparticles, particularly in aqueous media, aligning with environmentally friendly practices. During PISA, the chain extension of a hydrophilic polymer block with hydrophobic monomers triggers in situ self-assembly, yielding nanostructures such as spherical micelles, fibers, worm-like particles, vesicles, and lamellas.[1] Unlike traditional methods requiring volatile organic solvents, PISA offers a sustainable alternative for biomedical applications.[2] For the purpose of chain-extension, PISA is dominantly coupled with controlled polymerisation techniques, including Atom Transfer Radical Polymerisation, Nitroxide-Mediated Polymerisation, RingOpening Metathesis Polymerisation, and Ring-Opening Polymerisation, but predominantly with Reversible-Addition Fragmentation Chain Transfer (RAFT) polymerisation.[3–7] Typically, a hydrophilic macro-chain transfer agent (macroCTA) is synthesised in an organic solvent before initiating PISA.[8–11] While polyethylene glycol, poly(meth)acrylamides and poly(meth)acrylates are common macroCTAs, only few examples of alternatives are described in the literature.[12]

Polypeptoids, due to their structural similarity to natural polypeptides, are promising candidates for PISA-based biomaterials, offering biocompatibility, stability, and tunable functionality.[13–15] Polypeptoids can be synthesised via solidphase synthesis or through the ring-opening polymerisation of N-carboxyanhydrides.[16–18] These methods have been combined with PISA to produce water-soluble coronas or hydrophobic cores. However, while solid-phase synthesis is effective for short oligomers, it requires labor-intensive protection-deprotection steps, whereas ring-opening polymerisation demands complex monomer synthesis and stringent reaction conditions.[19] In contrast, the Ugi multicomponent reaction (Ugi MCR) provides an efficient route to obtain polypeptoids with atom economy, mild conditions, and broad structural diversity.[20–24] Extensively applied in various fields,[25–29] this approach has proven particularly useful for polymerisation of amino acids. For example, Zhang et al. synthesised γ-, δ-, and ε- polypeptoids from bifunctional amino acids for drug encapsulation,[30] while Debuigne's group developed alternating polypeptide-polypeptoid copolymers and explored their functionalisation.[31,32] Tao et al. further confirmed polycondensation nature of Ugi MCR, yielding to the formation of alternating polypeptoids and polyampholytes.[33] Among diverse polypeptoids that can be obtained by Ugi MCR, PεLL is of great interest for further investigation. Resulted from biosynthesis of various microorganism,[34,35] natural existing PεLL is known for its antimicrobial activity, heat stability and low

Published in : Polymer Chemistry (2025), vol. 16, n°26, pp. 3041–3050
DOI: 10.1039/D5PY00384A
Status : Postprint (Author's version)

toxicity. The functionalisation of PεLL has, thus, attracted a continuing interest for various applications in the medical field.[36–38] For this purpose, along with other chemosynthetic routes for functionalisation of PεLL,[30,39] Ugi MCR has emerged as a promising technique for synthesising polymers while enabling the introduction of new functionalities.

The combination of Ugi MCR with controlled radical polymerisation has been reported in the literature. For example, the group of Tao has described the use of Ugi MCR to graft polymers on carbon nanotubes,[40] to conjugate polymer with protein,[41] or to prepare miktoarm polymers[42] by RAFT polymerisation. Despite the efficiency of the Ugi MCR in polypeptoid synthesis, the use of Ugi MCR to prepare hydrophilic block for PISA-RAFT remains unexplored.

In this work, we demonstrate the one-pot synthesis of a macroCTA trithiocarbonate (TTC) derived from PεLL using the Ugi MCR, hereinafter referred to as PεLL-TTC. The obtained PεLL-TTC is characterised by various techniques (NMR, SEC, UV- Vis, MALDI-ToF) to confirm the chain-end fidelity and their molar mass. PεLL-TTC is then employed as hydrophilic block for chain extension with the hydrophobic HPMA in water at 55 °C with systematic changes in mass content and degree of polymerisation (DP) of the PHPMA block. Formation of particles are observed during the polymerisation and characterised by various analyses including dynamic light scattering (DLS), transmission electron microscopy (TEM), and when adapted small angle X-ray scattering (SAXS).

Experimental

MATERIALS

Unless otherwise stated, all chemicals are used as received. KOH (Sigma Aldrich), acetone (pure, Carlo Erba), ethanethiol (97% pure, Alfa Aesar), carbon disulfide (99.9%, Alfa Aesar), 4-toluenesulfonyl chloride (PTSC), dichloromethane (pure, stabilised with amylene, Carlo Erba), 4,4′-Azobis(4-cyanovaleric acid) (AICV, 98% pure, Sigma Aldrich), tert-butyloxycarbonyl-L- Lysine (Boc-Lys) (97% pure, Alfa Aesar), formaldehyde (37 wt% in water with 10-15% methanol as stabiliser, Thermo Scientific), tert-butyl isocyanide (98% pure, Sigma Aldrich or 97 %, Thermo Scientific), diethyl ether (pure, stabilised with BHT,), trifluoroacetic acid (99% pure, Thermo Scientific), 2,2'-Azobis(2- methylpropionamidine) dihydrochloride (V-50, granular, 99% pure, Aldrich), 2-hydroxypropyl methacrylate (HPMA, 98% pure, mixture of isomers, stabilised by 0.02% 4-methoxyphenol, Alfa Aesar), methanol (anhydrous, Carlo Erba). HPMA was filtered over silica gel to

Published in : Polymer Chemistry (2025), vol. 16, n°26, pp. 3041–3050
DOI: 10.1039/D5PY00384A
Status : Postprint (Author's version)

remove stabiliser before use.

METHODS SYNTHESIS OF 4-CYANO-4-[[(ETHYLTHIO)THIOXOMETHYL]THIO]PENTANOIC ACID (CEPA)

CEPA was synthesised as reported in the literature.[43] In brief, KOH (6.72 g, 0.07 mol) was dissolved in 25 mL of acetone:water (20:5 v/v) mixture in a round bottom flask. Ethanethiol (7.4 mL, 0.10 mol) was added to the mixture under stirring. The flask was then cooled down in an acetone bath following by the addition of carbon disulfide (6 mL, 7.61 g, 0.10 mol). After 45 minutes of stirring, PTSC (9.91 g, 0.052 mol) was added to the mixture then stirred at room temperature for 1 hour. The mixture was then heated to 45 °C and stirred for 30 minutes. The remaining was then diluted in 150 mL of dichloromethane and washed with 50 mL of distilled water (twice). The volatile compounds were eliminated by evaporation under a fume hood, and an orange crude product was obtained. AICV (15.2 g, 0.053 mol) was added to the crude product following by addition of 300 mL of ethyl acetate. The whole mixture was then degassed with argon, stirred then heated to 75 °C with reflux for 20 hours. The mixture was cooled down to room temperature, the solvent was then evaporated using a stream of argon. The final product was obtained by column chromatography on silica gel using a gradient solvent mixture of cyclohexane and dichloromethane with >99% dichloromethane at the end. The purified product was obtained as an orange solid after evaporation of solvent. ^{1}H-NMR: DMSO-d6, 400 Hz, δ: 1.36 ppm (triplet, 3H, CH3-CH2-), 1.88 ppm (singlet, 3H, CH3-C(CN)-), 2.40-2.53 ppm (m, 2H, - C(CN)-CH2-), 2.69 ppm (m, -CH2-COOH), 2.35ppm (quartet, 2H, CH3-CH2-S-C(=S)-S)).

SYNTHESIS OF BOC-PƐLL-TTC

In a 10-mL round bottom flask, CEPA (0.10 g, 0.38 mmol, 0.05 eq.) was weighed followed by Boc-Lys (1.78 g, 7.21 mmol, 0.95 eq.) then 8 mL of methanol:H2O (1:1 v/v) was added then the mixture was stirred using a magnetic bar. Formaldehyde (9.87 mmol, 1.3 eq.) was added to the mixture using a micropipette resulted in full dissolution of all solids. Finally, with precaution, tert-butyl isocyanide (9.87 mmol, 1.3 eq.) was added dropwise to the reaction mixture using a micropipette. The flask was secured and close with a septum. The reaction was proceeded at room temperature. After 24 hours, phase separation was observed. The polymers (Boc-PƐLL-TTC) were isolated by discarding the transparent aqueous phase. The crude polymer was then diluted in methanol prior to precipitation in cold diethyl ether. After filtration through a Büchner funnel under reduced pressure, a light-yellow

Published in : Polymer Chemistry (2025), vol. 16, n°26, pp. 3041–3050
DOI: 10.1039/D5PY00384A
Status : Postprint (Author's version)

powder was obtained and subsequently dried under vacuum to yield purified Boc-PεLL- TTC (yield: 30%).

DEPROTECTION OF BOC-PεLL-TTC TO OBTAIN PεLL-TTC

400 mg of Boc-PεLL-TTC was charged into a 10-mL round bottom flask with a stirring bar. The polymer was dissolved in molecular-sieve-dried 1 mL dichloromethane. The flask was then immersed in an ice bath. 1 mL of trifluoroacetic acid was added dropwise to the reaction mixture. After 3–4 hours, the reaction mixture was concentrated by rotary evaporation. The PεLL-TTC polymer was retrieved by precipitation in cold diethylether and dried under vacuum to obtain light yellow powder (yield: 90%).

PISA-RAFT CHAIN EXTENSION OF PεLL-TTC WITH HPMA

A typical PISA-RAFT chain extension of PεLL-TTC with HPMA was carried out as follows : For a target degree of polymerisation (DP_0) of 200 and a polymerisation at 5 wt% in monomer: 10 mg of PεLL-TTC (Mn, UV = 2900 $g.mol^{-1}$, 5 x 10^{-3} mmol) was weighed into a vial. Then 2.550 mL miliQ water was added to dissolve the macroCTA followed by addition of 0.250 mL aqueous solution containing 0.27 mg V-50. Finally, 0.140 mL of HPMA was added into the reaction mixture. The vial was then closed with a silicon septum. The reaction mixture was stirred and degassed with moderate flow of argon for 15 minutes. After degassing, the polymerisation commenced as soon as it was immersed in a preheated oil bath at 55 °C. The polymerisation was quenched

by exposure to air after 21 hours of reaction, with >90% monomer conversion confirmed by ^{1}H NMR analysis.

KINETICS OF PISA-RAFT CHAIN EXTENSION OF PεLL MACROCTA WITH HPMA

The kinetics of chain extension of PεLL2.9K macroCTA with HPMA in water was performed at DP0 = 100, 5 wt% in a 5-mL vial. First, 10.8 mg V-50 was dissolved in 10mL of milliQ water as stock solution. 0.5 mL of the initiator stock solution (0.54 mg V-50, 2.0 x 10^{-6} mol, 0.2 eq) was transferred into a vial containing 29 mg of PεLL2.9K (1.00 x 10^{-5} mol, 1.0 eq.) and a magnetic stirring bar. 2.30 mL of milliQ water was adjusted to the vial following by addition of 0.140 mL of HPMA (0.144 g, 1.00 x 10^{-3} mol, 100 eq., 5 wt%). The vial was closed with a silicone septum and degassed with argon in 15 minutes at room temperature. Argon was removed at the end of degassing and the vial was sealed with

Published in : Polymer Chemistry (2025), vol. 16, n°26, pp. 3041–3050
DOI: 10.1039/D5PY00384A
Status : Postprint (Author's version)

parafilm then immersed in preheated oil bath at 55 °C to start the kinetics. An aliquot (200 µL) of reaction mixture was taken in a regular interval using a degassed disposable syringe for NMR, SEC, and DLS analyses.

Characterisation

NMR SPECTROSCOPY

NMR was carried out using Bruker 400 MHz spectrometer. Polymer concentration was of 20 mg per 1 mL deuterated solvent and measurement was carried out in 5-mm tube. The spectra were analysed using MestReNova 5.3.0 (Mestrelab Research S.L.). Chemical shifts are reported in ppm.

SIZE EXCLUSION CHROMATOGRAPHY

Molar mass determination of polymers was obtained using size exclusion chromatography (SEC) in DMF (+ NH4BF4 5 mM) as the eluent at 50 °C. SEC analyses were performed on a Shimadzu instrument fitted with mixed-C columns and RI detector. Molar mass in number (Mn), molar mass in weight (Mw) and molar (PEG) standards with molecular weight in the range of 610 g

mol^{-1} to 1 511 0000 g mol^{-1}.

UV-VISIBLE SPECTROSCOPY

Absorbance measurements of solutions were performed using an Agilent Cary 60 UV-Vis spectrophotometer at room temperature. Calibration curve of CEPA was constructed from various solution obtained by dilution a stock solution of pure CEPA in methanol.

DLS/ZETA POTENTIAL

Dynamic Light Scattering (DLS) and zeta potential measurements were performed on Malvern Zetasizer Nano S instrument at 25 °C. All measurements were performed on diluted dispersion at 0.03 wt% in milliQ water. Z-average hydrodynamic diameters (DZ) and polydispersity (PDI) were calculated from 3 repeat measurements using the Stokes-Einstein equation, which assumes perfectly monodisperse, non-interacting spheres.

Published in : Polymer Chemistry (2025), vol. 16, n°26, pp. 3041–3050
DOI: 10.1039/D5PY00384A
Status : Postprint (Author's version)

TRANSMISSION ELECTRON MICROSCOPY (TEM)

Dry-state transmission electron microscopy (TEM) imaging was performed on either FEI TECNAI F20 microscope at an S3 acceleration voltage of 200 kV. All aqueous samples were diluted in milliQ water to 0.03-0.05 wt% and then deposited onto formvar/carbon film coated copper grids (400 mesh). After 90s, excess sample was blotted from the grid and the grid was stained with an aqueous 1 wt% uranyl acetate (UA) solution for 1 min prior to blotting, drying and microscopic analysis.

Scheme 1. *General strategy for the synthesis of poly(ε -L-Lysine) Pε LL-decorated nanoparticles by sequential Ugi polymerization and PISA- RAFT polymerisation in water*

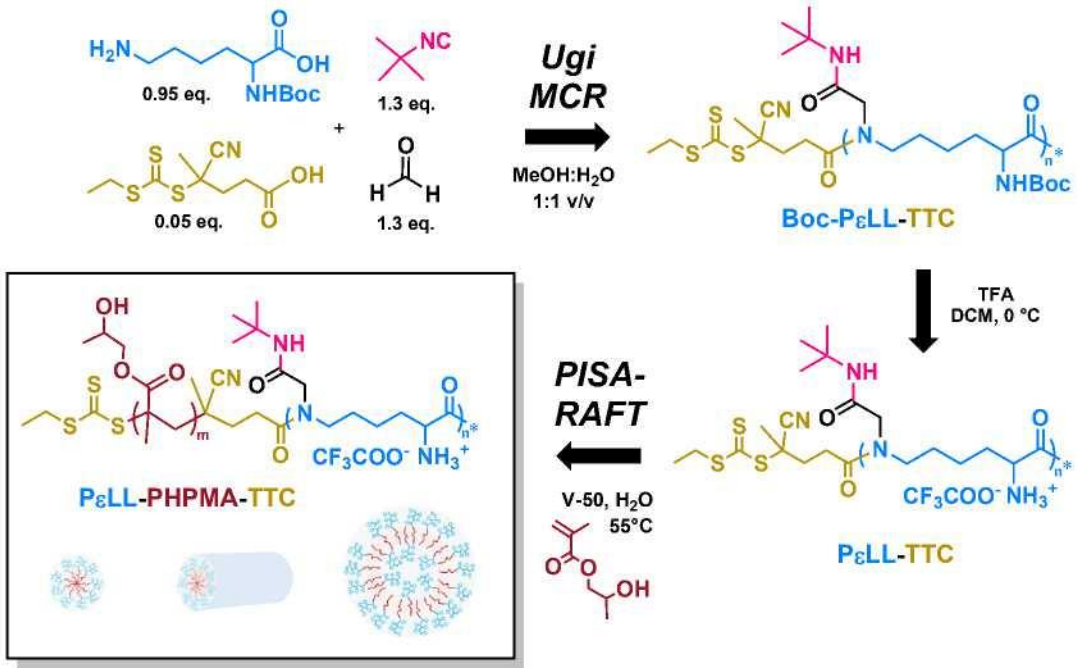

mass dispersities (Đ) were calculated using poly(ethylene glycol)

Results and discussion

In preliminary experiments, the synthesis of non-modified Boc- PεLL by Ugi MCR of Boc-Lys (1.0 eq.) with tert-butyl isocyanide (1.3 eq.) and formaldehyde (1.3 eq.) in MeOH/water (1/1 v/v) was performed for 24 hours, 48 hours and 96 hours. Obtained results (Table S1) show that higher molar masses can be obtained by extending reaction duration. However, the molar mass of obtained polymers remains limited (Mn < 5.0 kg mol^{-1}). This is probably due to presence of side-reaction that form a six-membered ring which is unable to propagate during polymerisation, as mentioned in the literature.[30]

Published in : Polymer Chemistry (2025), vol. 16, n°26, pp. 3041–3050
DOI: 10.1039/D5PY00384A
Status : Postprint (Author's version)

Inspired by our report on the chain-end functionalisation of polypeptoids,[32] the synthesis of the macro-RAFT agent was achieved in a single step by addition of a CTA during Ugi polymerisation of Boc-lysine (Boc-Lys) (Scheme 1). The CEPA/Boc-Lys molar ratio was fixed at 0.05:0.95 throughout the present work. The resulting Boc-PεLL-TTC was purified by precipitation in cold diethylether. The removal of Boc- protecting group was performed afterward in mixture of dichloromethane/trifluoroacetic acid (1:1 v/v). Table 1 summarises macromolecular characteristics of two Boc-PεLL- TTCs and their corresponding PεLL-TTCs used in the present work. Molar mass distributions of these polymers are shown in Figure 2. Molar mass of resulting Boc-PεLL-TTC is in the same range as of Boc-PεLL obtained without addition of CEPA under similar reaction conditions (24-hour or 48-hour hours).

Table 1 *Macromolecular characteristics of Boc-PεLL-TTC (entries a) and their corresponding PεLL-TTC (entries b) obtained after Boc-deprotection*

Entry	macroCTA	$M_{n,\,UV}$[a] (g.mol^{-1})	SEC[b]		
			$M_{n,\,SEC}$ (g.mol^{-1})	$M_{w,\,SEC}$ (g.mol^{-1})	$Đ$
1a*	Boc-PεLL$_{1.5K}$-TTC	1 800	2 300	4 200	1.82
1b	PεLL$_{1.5K}$-TTC	1 500	6 700	8 900	1.36
2a**	Boc-PεLL$_{2.9K}$-TTC	2 100	4 500	6 000	1.35
2b	PεLL$_{2.9K}$-TTC	2 900	10 900	13 400	1.23

*24-hour reaction, ** 48-hour reaction

[a] determined by UV-Vis absorption of TTC, [b] eluent: DMF + 5mM NH4BF4 at 50 °C, PEG calibration

Figure 1 shows ^{1}H-NMR spectra of Boc-PεLL, Boc-PεLL-TTC and CEPA. The addition of CEPA into Ugi MCR of Boc-Lys successfully results in Boc-PεLL-TTC as confirmed by the presence of the methyl peak g originated from CEPA at around 1.9 ppm, which is absent from pure Boc-PεLL. Furthermore, characteristic signals of Boc-PεLL are present with methylene protons of the PεLL and methyl protons of the tert-butyl groups located from 1.0 ppm to 1.6 ppm. Protons adjacent to amide functions are found between 2.8 ppm and 4.4 ppm whereas protons of amide functions are present between 6.2-7.8 ppm. In addition, ^{13}C- NMR spectrum of these three materials (Supplementary Information, Figure S1) also indicates a characteristic peak of a methyl carbon at 12.8 ppm which is

Published in : Polymer Chemistry (2025), vol. 16, n°26, pp. 3041–3050
DOI: 10.1039/D5PY00384A
Status : Postprint (Author's version)

observed in CEPA yet absent in Boc-PεLL. Unfortunately, other characteristic peaks of CEPA are not observable in the ^{1}H-NMR spectrum for they are obscured by overlapping signals from Boc-PεLL.

***Figure 1**. ^{1}H-NMR spectrum of a) Boc-PεLL, (b) Boc-PεLL-TTC, and (c) pure CEPA in DMSO-d**6** confirming the success in synthesis of Boc-PεLL-TTC by UGI multicomponent reaction, *indicate residual solvent.*

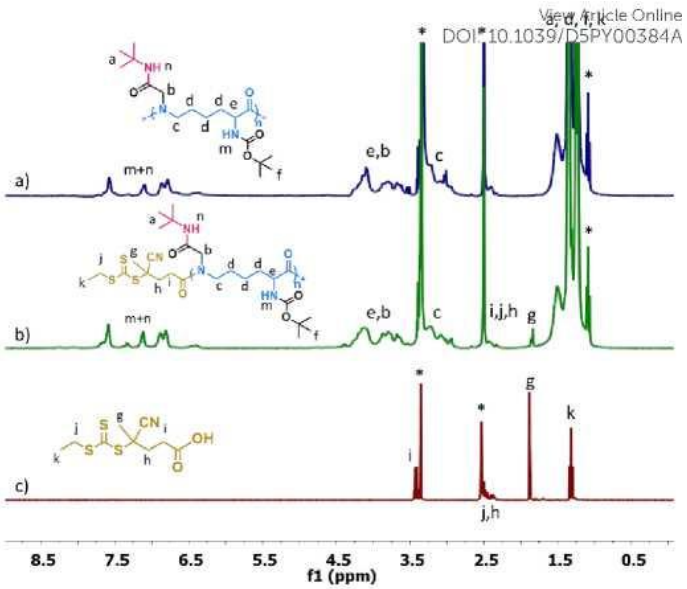

For further investigation, MALDI-ToF analysis was performed on two Boc-PεLL-TTC macroCTAs (Supplementary Information, Figure S2). Obtained results confirm the integrity of the polymer structure given by a series of peaks with Δ (m/z) ≈ 341 corresponding to a repeating unit of Ugi derivatives Boc-PεLL. More importantly, evidence on the presence of trithiocarbonate function was also seen from MALDI-ToF results (yellow triangle species, Supplementary Information, Figure S2). However, the signals from those species are less intense probably due to the sensibility of trithiocarbonate functions to MALDI measurement as reported elsewhere.[44]

To result in a water soluble PεLL-TTC, the Boc protecting group was removed in mixture of dichloromethane/trifluoroacetic acid (1:1 v/v) at 0 °C for 3-4 hours.

Published in : Polymer Chemistry (2025), vol. 16, n°26, pp. 3041–3050
DOI: 10.1039/D5PY00384A
Status : Postprint (Author's version)

Figure 2. *Molar mass distribution of different Boc-PεLL-TTC and PεLL-TTC given in Table 1. SEC measurements were performed in DMF (+ NH**4**BF**4** 5 mM) at 50 °C with PEG calibration*

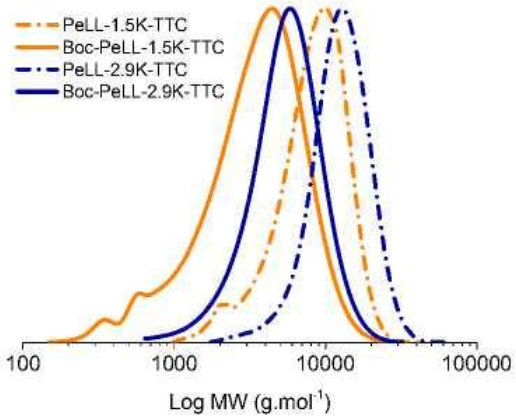

The disappearance of signals at 1.3 ppm in ^{1}H-NMR of polymers after deprotection and purification (Supplementary Information, Figure S3) indicates successful quantitative elimination of the Boc protecting group. In accordance, ^{19}F- NMR shows presence of trifluoroacetate counterions (Supplementary Information, Figure S4). ^{13}C-NMR further confirms the disappearance of peaks originated from tert-butyl group after Boc deprotection (Supplementary Information, Figure S5).

Molar masses of PεLL-TTC were then characterised by chain-end analysis via UV-Vis absorption and size exclusion chromatography (SEC). Results of these analyses are summarised in Table 1. First, quantification of TTC by UV-Vis absorption at λ = 305 nm in methanol was performed based on a calibration curve of pure CEPA (Figure S6, Supplementary Information). Mn, UV can be deduced from the concentration of TTC as given by Equation 1 (Supplementary Information) assuming that each polymer chain bears one TTC. As expected, polymers obtained from Ugi MCR over 48-hour reaction have higher molar mass, 2100 g.mol^{-1} for Boc-PεLL-TTC (Entry 2a, Table 1) and 2900 g.mol^{-1} for PεLL-TTC (Entry 2b, Table 1) in comparison to 1800 g.mol^{-1}(Entry 1a, Table 1) and 1500 g.mol^{-1} (Entry 1b, Table 1), respectively, for those obtained over 24 hours. SEC in DMF (+ 5mM NH_4BF_4 with PEG calibration) was also performed to obtain relative Mn,SEC and dispersity of Boc- PεLL-TTC as well as PεLL-TTC, as shown in Figure 2. Obtained results from SEC and UV-Vis confirm the difference in molar mass at varied Ugi MCR reaction time, i.e. longer the reaction, greater the chain length. However, Mn,UV is smaller than Mn,SEC for all studied polymers, which is expected because calculation of Mn,UV was performed by assuming 100% chain-end functionalisation. Furthermore, Mn,SEC was obtained as relative Mn with PEG calibration in DMF. As the chain-end functionalisation of the PεLL

Published in : Polymer Chemistry (2025), vol. 16, n°26, pp. 3041–3050
DOI: 10.1039/D5PY00384A
Status : Postprint (Author's version)

was carried out in situ during the polycondensation reaction, there are possibly non-functionalised Boc-PεLL mixed with functionalised Boc-PεLL- TTC. The difference between Mn,UV and Mn,SEC is particularly significant for the cationic PεLL-TTC. This is because in SEC measurement, the charged nature of PεLL-TTC causes Mn,SEC to shift to higher molar mass. This shift can be attributed to the altered interaction of the polymers with the column material. Nevertheless, Mn,UV before and after Boc-deprotection of the same polymer remains in the same range of molar mass, indicating TTC group remains intact after deprotection with trifluoroacetic acid. Due to the importance of quantifying TTC in the subsequent RAFT-PISA process, Mn,UV was used as the reference value for further experiments. The macroCTA are therefore denoted by their corresponding Mn,UV as PεLL1.5K-TTC and PεLL2.9K-TTC.

The resulting hydrophilic PεLL-TTC then served as macroCTAs in the aqueous RAFT polymerisation of HPMA at 55 °C (see Scheme 1). Table 2 summarises results on chain extension of $PεLL_{1.5K}$-TTC with HPMA in water at 55 °C for 20 hours of reaction using V50 as initiator. Under studied conditions, monomer conversion was >90 % for all experiments with most achieving quantitative conversion. Molar mass after RAFT polymerisation of final formulations was analysed by SEC. These results are presented in Figure S7, Supplementary Information. Overall, except for DP0 = 70, the increase in DP0, PHPMA gave rise to molar mass of obtained copolymers, featuring efficient chain extension. Though the inevitable presence of non-functionalised PεLL is noticed for all experiments, these signals reduced in intensity when higher DP are expected.

Published in : Polymer Chemistry (2025), vol. 16, n°26, pp. 3041–3050
DOI: 10.1039/D5PY00384A
Status : Postprint (Author's version)

Table 2. *Summary of PεLL$_{1.5K}$-TTC chain extension with HPMA by RAFT polymerisation in aqueous medium. Polymerisation condition: [macroCTA]0:[V-50]0 = 1/0.2, T = 55 °C, t = 21h, %wt: mass content of HPMA in water, DP0 = [PεLL-TTC]0/[HPMA]0*

Entry	%wt	DP_0	Conv. (%)	DP_{NMR}	$M_{n,theo}$* (g.mol^{-1})	$SEC_{DMF, PEG\ calibration}$			TEM**	DLS	
						$M_{n,SEC}$* (g.mol^{-1})	$M_{w,SEC}$ (g.mol^{-1})	$Đ$		Z-ave (d, nm)	PDI
P1	5	10	>99	10	2 900	12 700	25 700	2.02	sS, sW	235	0.29
P2		20	>99	20	4 380	18 800	65 800	3.49	S	310	0.02
P3		30	>99	30	5 820	17 300	99 500	5.74	S	376	0.01
P4		50	91	46	8 052	28 300	163 200	5.78	V	583	0.07
P5		70	97	68	11 278	27 000	115 300	4.28	V	468	0.02
P6	10	10	>99	10	2 940	11 600	19 300	1.67	sS,sW	45	0.19
P7		20	>99	20	4 380	19 400	69 700	3.59	S	881	0.22
P8		30	>99	30	5 820	16 400	75 400	4.60	V	730	0.21
P9		50	>99	50	8 700	22 700	151 800	6.69	V	666	0.07
P10		70	>99	70	11 580	27 700	140 900	5.08	V	769	0.26
P11	15	10	>99	10	2 940	11 400	18 000	1.58	sS,sW	73	0.12
P12		20	>99	20	4 380	18 400	49 200	2.67	V	1934	0.63
P13		30	>99	30	5 820	18 000	99 500	5.57	V	1383	0.68
P14		50	>99	50	8 700	29 100	160 300	5.52	V	1444	1.00
P15		70	98	69	11 378	31 500	131 700	4.18	-	-	-

*: Mn, theo was calculated from conversion determined by 1H-NMR and from Mn, UV, **: expected morphology: sS = small sphere, S = sphere, sW = short worm-like particle, V = vesicle

At the end of polymerisation, except for DP0 = 70 at 15 wt%, final solutions were obtained as a stable dispersion given by their visual appearance (Figure S8). As is typical in the PISA process, nanoparticles are formed progressively as the polymerisation proceeds. Their formation causes light scattering, resulting in a transition to a turbid or milky-white appearance. Digital photos of polymer solutions, DLS results and TEM images of final formulation can be found in Supplementary Information, Figure S8, Figure S9 and Figure S10, respectively. Figure 3a illustrates the phase diagram of PεLL$_{1.5K}$-b-PHPMA in function of monomer content and DP_0 with representative TEM images of different morphologies obtained during PISA process. Overall, various morphologies were obtained from PεLL$_{1.5K}$-TTC by PISA-RAFT process with HPMA at 5 wt%,10 wt% or 15 wt% monomer content. First of all, at DP_0 = 10, based on visual appearance of final formulation, an evolution in morphology was expected with turbid solution (5 wt%) giving spherical micelles, viscous solution at 10 wt% giving mixture of spheres and short worm-like particles, and only gel at 15 wt% giving fiber structure. By TEM, mixture of small spheres and short worm-like particles are observed from these three formulations. Unusual globular morphologies that appear intermediate or ill-defined may arise from the short HPMA chains used in these experiments may result in an unstable packing parameter, preventing the system from reaching well- defined equilibrium morphologies. Higher

Published in : Polymer Chemistry (2025), vol. 16, n°26, pp. 3041–3050
DOI: 10.1039/D5PY00384A
Status : Postprint (Author's version)

resolution TEM images of the short worm-like structures are presented in Figure S10. In agreement, DLS results show large polydispersity and significant deviation in particles' size among number,

intensity and volume signals. The difference in expected morphology and TEM image could be attributed again to the very short hydrophilic or HPMA block, which may cause instability upon dilution for TEM preparation, as reported in the literature for short poly(α-lysine) used as a macroCTA.[45] Specifically, as reported in the literature, nanostructures derived from short poly(α-lysine) (~780 $g.mol^{-1}$) have been shown to lose stability upon dilution, leading to poorly defined structures observed in post-experiment TEM and DLS analyses. On the other hand, at a fixed monomer content of 5 wt%, as the proportion of DPHPMA increases, the morphology evolution of the diblock system was observed. In comparison to DP = 10, when PHPMA block has DP = 20 or DP = 30, well-defined spherical structures were seen under TEM with DLS giving Z- average of 300-370 nm and PDI = 0.01-0.02; at DP ~ 50, a clear donut-type vesical structure was observed in TEM. At higher monomer content, 10 wt% for examples, the same phenomenon is observed with changes between DPPHPMA = 10 and higher DPPHPMA. At DP = 70, a clear vesicle structure was seen in TEM images. Interestingly, when DPPHPMA ≥ 20, the change in nanoparticles size appear to be mostly dependent on monomer content rather than DP of PHPMA block. As expected, as the hydrophobic core gets bigger, the stability of the system is lost given by the formation of unstable aggregates and eventually precipitates are observed visually in the final solution.

To explore the effect of PεLL chain length on the PISA process, another series of experiments was performed with PεLL2.9K. Longer stabilising block is expected to form more stable nanoparticles with certain changes in particle sizes. Table S3 (Supplementary Information) summarises results on chain extension of PεLL2.9K-TTC with HPMA in aqueous condition. Digital photos of final appearances of these formulations are presented in Figure S12 (Supplementary Information). Figure 3b shows phase diagram and TEM images of acquired formulations. Overall, compared to PεLL1.5K-TTC, the conversion of HPMA was lower, especially when high DP0 or high monomer concentration was targeted. In SEC profiles presented in Figure S11, molar masses achieved with the use of PεLL2.9K-TTC also increased with increase in target DPHPMA. However, at 15 wt% and DP ≥ 150 (P26, P27, Table 3), precipitation was observed at 50-60% monomer conversion and SEC analysis was not performed as the polymer solution cannot be filtered over 0.45 µm filter. Similar to PεLL1.5K-TTC, residual of non-functionalised PεLL was present in all formulations.

Published in : Polymer Chemistry (2025), vol. 16, n°26, pp. 3041–3050
DOI: 10.1039/D5PY00384A
Status : Postprint (Author's version)

Figure 3. *Phase diagrams and representative TEM images of nanoparticles obtained by PISA-RAFT chain extension of a) PεLL1.5K macroCTA and b) PεLL$_{2.9K}$ macroCTA with HPMA in aqueos medium where DP$_0$ and monomer content were varied. The scale bar is of 1 µm for PεLL$_{1.5K}$ macroCTA and 0.5 µm for PεLL$_{2.9K}$ macroCTA. Abbreviation: sS = small sphere, sW = small worm-like particle, S = sphere, V = vesicle, P = precipitation*

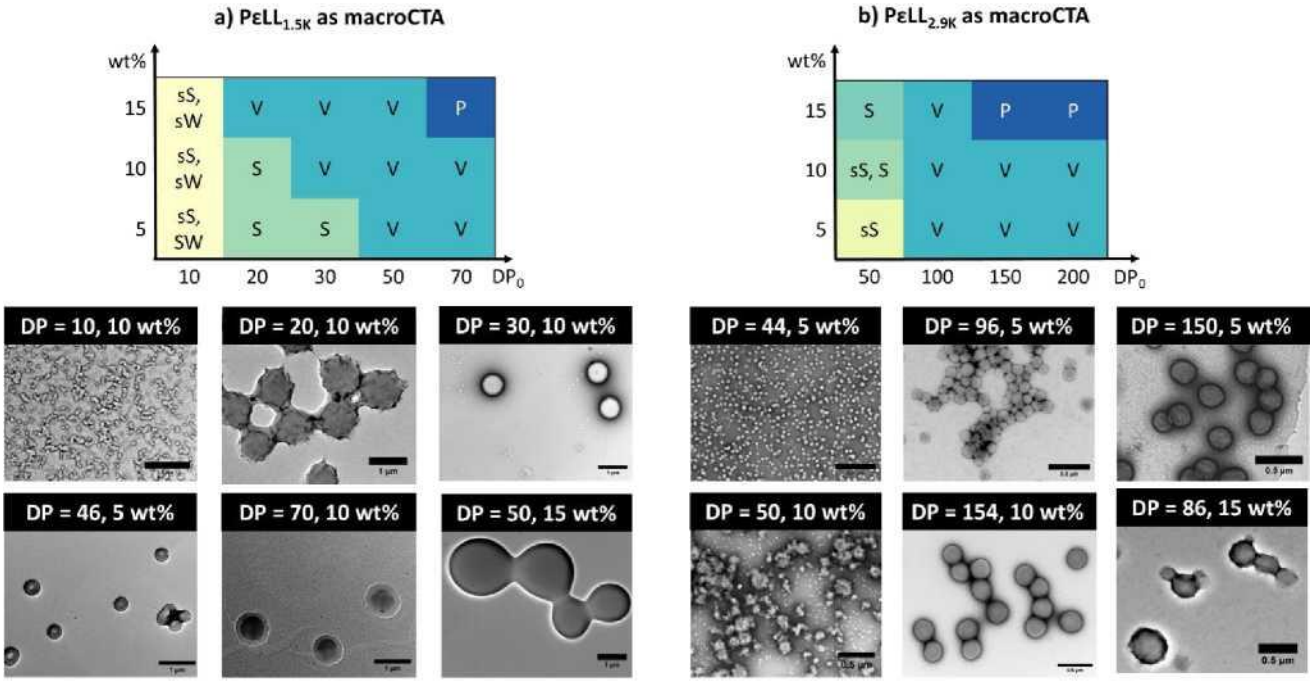

Table 3. *Summary of PεLL$_{2.9K}$-TTC chain extension with HPMA by RAFT polymerisation in aqueous medium. Polymerisation condition: [macroCTA]0:[V-50]0 = 1/0.2, T = 55 °C, t = 21h, %wt: mass content of HPMA in water, DP0 = [PεLL-TTC]0/[HPMA]*

Entry	%wt	DP$_0$	Conv. (%)	DP$_{NMR}$	M$_{n,theo}$* (g.mol^{-1})	SEC$_{DMF, PEG\ calibration}$			TEM**	DLS	
						M$_{n,SEC}$ (g.mol^{-1})	M$_{w,SEC}$ (g.mol^{-1})	Đ		Z-ave (d,nm)	PDI
P16	5	50	>99	44	9 240	18 800	42 500	2.26	sS	92	0.25
P17		100	87	96	16 740	31 500	124 700	4.00	sS, S	188	0.12
P18		150	>99	150	24 530	33 000	136 500	4.14	S	283	0.02
P19		200	>99	200	31 740	29 700	84 400	2.84	V	123	0.06
P20	10	50	>99	50	10 110	72 300	344 000	4.76	V	254	0.02
P21		100	80	80	14 430	57 100	187 000	3.28	V	396	0.03
P22		150	88	132	21 930	17 500	85 100	4.88	V	463	0.07
P23		200	77	154	25 100	84 700	417 200	4.93	V	319	0.04
P24	15	50	96	48	9 820	21 700	53 400	2.46	V	374	0.20
P25		100	85	85	15 160	30 100	142 100	4.72	V	377	0.06
P26		150	57	86	15.300	NA	NA	NA	-	-	-
P27		200	51	102	17 610	NA	NA	NA	-	-	-

*: Mn, theo was calculated from conversion determined by 1H-NMR and from Mn, UV - **: expected morphology, sS = small sphere, S = sphere, sW = short worm-like particle, V = vesicle, NA: measurement was not performed due to impossibility of filtration

Published in : Polymer Chemistry (2025), vol. 16, n°26, pp. 3041–3050
DOI: 10.1039/D5PY00384A
Status : Postprint (Author's version)

In term of morphology, unlike PεLL1.5K-PHPMA where some small worm-like particles can be found at low DP, only spherical structures were found for PεLL2.9K-b-PHPMA system, which was also described in the literature for other ionic diblocks obtained by PISA-RAFT in aqueous medium.[46–48] As seen in Figure 3b and Figure S14, at DP ~ 50, small spheres and mixture of spheres with varied size were found at 5 wt% and 10 wt%. At higher DPHPMA, the particle sizes increase significantly. As expected, the size of nanoparticles based on PεLL2.9K-PHPMA is about twice as small as that obtained by PεLL1.5K-PHPMA due to longer stabilizer block.

To assess the stability of nanoparticles, zeta-potential measurement was performed for formulations at 10 wt% monomer content. As seen in Figure S15, as expected, all nanoparticles show positive zeta potential due the cationic nature of PεLL as stabilising block. Furthermore, the zeta potential of obtained nanoparticles increases gradually with an increase of PHPMA block length. When the DPHPMA < 140, all nanoparticles have zeta-potential between 45-55 mV, indicating good colloidal stability of ionic particles. However, at DPHPMA = 154, the zeta potential of nanoparticles drops to ~22 mV, indicating the loss in ionic stability. This result is consistent with visual observation where aggregation was found on the formulation of PεLL2.9K-PHPMA154.

SAXS analysis was performed for samples whose characteristic size observed in TEM was smaller than 50 nm including PεLL1.5K- PHPMA10 and PεLL2.9K-PHPMA50 prepared at 5 wt% and 10% monomer content. For each of these samples, the scattering intensity as a function of wave vector is shown in Figure S16, Supplementary Information. The data was analysed in agreement with the TEM data and images using polydisperse hard spheres (Equation 2, Supplementary Information). The fitting results are of good agreement with TEM and DLS analyses as given in Table S4, Supplementary Information.

Finally, the kinetics of chain extension were studied on PεLL2.9K with a target degree of polymerisation DP0 = 100 and 5 wt% solids content, to investigate the process kinetics during PISA-RAFT, as summarised in Figure 4. As seen in Figure 4a, under studied conditions, the chain extension of PεLL2.9K-TTC with HPMA took place quite rapidly and reached >90% monomer conversion after ~70 minutes. An onset of polymerisation was observed around 35 minutes, which is consistent with visual observation where a rapid change in solution appearance from transparent to turbid was observed between 30 minutes and 45 minutes. Figure S17a (Supplementary Information) presents global molar mass evolution during the kinetic.

Published in : Polymer Chemistry (2025), vol. 16, n°26, pp. 3041–3050
DOI: 10.1039/D5PY00384A
Status : Postprint (Author's version)

Figure 4. *Kinetics of chain extension of PεLL2.9K macroCTA with HPMA (DP0 = 100) at 5 wt% in terms of a) conversion over reaction time and pseudo-first linear plot, b) molar mass and polydispersity evolution from SEC measurements with exclusion of non-functionalised PεLL residuals, and c) size evolution of formed nanoparticles over time by DLS measurement*

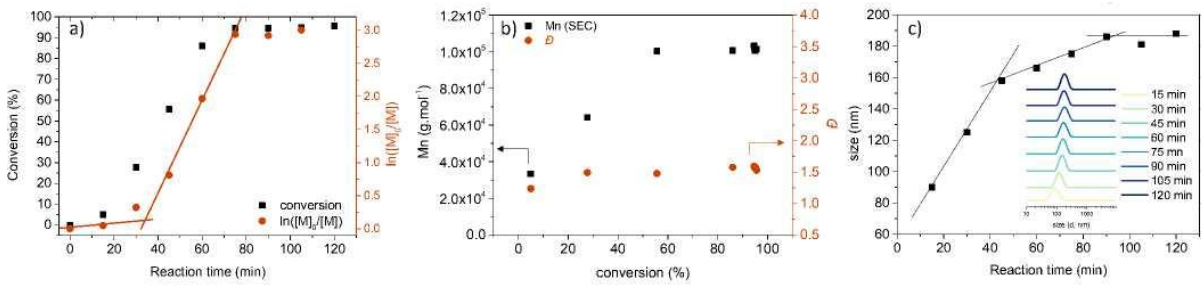

It is seen that after 15 minutes (5% monomer conversion determined by ^{1}H- NMR), a second population appears on SEC profiles, which takes ~15% of the whole molar mass distribution. As the monomer conversion increases with reaction time, a linear increase in molar mass was obtained until ~50% monomer conversion given by the shift to higher molar mass of the second population in the SEC profiles. Nonetheless, above 50% monomer conversion, no clear shift was observed. As discussed previously, as the PεLL is positively charged, certain interaction with column materials could occur, leading to difficulty in molar mass separation.[47] Even though a bimodal molar mass distribution was observed due to the presence of non-functionalised PεLL, by excluding non-functionalised PεLL from the molar mass determination of the diblock, the molar mass distribution appears monomodal, and the weight fraction of this population (Figure S17b, Supplementary Information) increases with monomer conversion. The molar mass dispersity of obtained diblock copolymers also stays around 1.5, featuring a relative controlled polymerisation.

In terms of size evolution as presented in Figure 4c, the diameter of nanoparticles increases with reaction time and monomer conversion. Three regimes can be observed in the evolution of nanoparticles size. The first regime corresponds to the onset of polymerisation, with the initial formation of nanoparticles observed when monomer conversion is below 30%. Even at low monomer conversion of ~5% at 15 minutes, small particles of ~90 nm were already formed and increase to ~125 nm at ~25% monomer conversion. After 35 minutes, as shown in Figure 4a, micelle structures are formed and gradually increase in size due to increase in monomer conversion. Once the monomer conversion is >90%, almost no change in particles size was observed by DLS. TEM images taken for solution at 5%, 55.6% and 95.6% monomer conversion (Figure S18, Supplementary

Published in : Polymer Chemistry (2025), vol. 16, n°26, pp. 3041–3050
DOI: 10.1039/D5PY00384A
Status : Postprint (Author's version)

Information) also confirms the evolution in particle sizes obtained by DLS.

Lastly, the presence of non-functionalised PεLL is consistently observed throughout this work. This is inevitable, as during the Ugi MCR polymerisation, CEPA competes with the carboxylic acid group of Boc-Lys rather than being selectively incorporated. Technically, due to the similar molar masses of non-functionalised PεLL and PεLL-TTC, separating them using conventional purification methods such as dialysis, precipitation, or centrifugation poses a major challenge. Nonetheless, for the particles' formation during PISA process, these non-functionalised PεLL appears to act as a co-stabiliser for the PεLL-PHPMA system with prospective ionic interaction between the charges, proven by a low to very low PDI (0.02-0.25) obtained by DLS measurements. Further study to synthesise PεLL-TTC with better chain-end fidelity may provide deeper insights on the role of non-functionalised PεLL on the self-assembly of PεLL-PHPMA during PISA process, which is essential regarding application of this system in biological fields.

Conclusions

In conclusion, this work provides a proof of concept for the successful one-pot synthesis of hydrophilic polypeptoids via the Ugi multicomponent reaction (MCR), using PεLL-TTC as a macroCTA for the PISA-RAFT process. The chain extension of PεLL-TTC with HPMA in aqueous medium proceeds as a controlled polymerisation, despite the presence of non-functionalised PεLL in the formulation, which shows minimal interference with the formation of PεLL-HPMA nanoparticles. Nanoparticles of various morphologies (small spheres, small approach. Furthermore, the size of these nanoparticles was demonstrated to depend on target DPHPMA,0 and monomer content as demonstrated by DLS results. In addition, zeta potential measurements showed a good stability of the formed particles and confirmed the ionic colloidal stabilisation nature of PεLL featuring by zeta-potential values between 45-55 mV. Given the combinatorial versatility of the Ugi MCR to prepare polypeptoids, with the robustness of PISA-RAFT in producing nanoparticles with diverse morphologies and tuneable sizes, this novel combination of Ugi MCR and PISA is expected to advance the synthesis and self-assembly of novel functional macromolecules.

Published in : Polymer Chemistry (2025), vol. 16, n°26, pp. 3041–3050
DOI: 10.1039/D5PY00384A
Status : Postprint (Author's version)

AUTHOR CONTRIBUTIONS

The manuscript was written through contributions of all authors. All authors have given approval to the final version of the manuscript.

CONFLICTS OF INTEREST

There are no conflicts to declare.

DATA AVAILABILITY

All raw data generated and analyzed during the course of this study, entitled "Poly(ε-L-Lysine)-Decorated Particles by Combination of Ugi Multicomponent Reaction and PISA-RAFT Polymerization", are securely stored at the Institut de Chimie et des Matériaux Paris-Est (ICMPE), CNRS. This includes all experimental procedures, nuclear magnetic resonance (NMR) spectroscopy data, dynamic light scattering (DLS) measurements, transmission electron microscopy (TEM) images, size exclusion chromatography (SEC) data, and other relevant characterization files supporting the results and conclusions presented in the manuscript.

These datasets are not publicly accessible. However, they are available from the corresponding author upon request.

ACKNOWLEDGEMENTS

This work was supported by financial funding from CNRS INC Emergence. We also acknowledge the support of the CAP and MIC ICMPE platforms, DIM MaTerRe, and the Île-de-France region.

DATA AVAILABILITY STATEMENT

All raw data generated and analyzed during the course of this study, entitled "Poly(ε-L-Lysine)-Decorated Particles by Combination of Ugi Multicomponent Reaction and PISA-RAFT Polymerization", are securely stored at the Institut de Chimie et des Matériaux Paris-Est (ICMPE), CNRS. This includes all experimental procedures, nuclear magnetic resonance (NMR) spectroscopy data, dynamic light scattering (DLS) measurements, transmission electron microscopy (TEM) images, size exclusion chromatography (SEC) data, and other relevant characterization files supporting the results and conclusions presented in the manuscript.

These datasets are not publicly accessible. However, they are available from the corresponding author upon request.

Published in : Polymer Chemistry (2025), vol. 16, n°26, pp. 3041–3050
DOI: 10.1039/D5PY00384A
Status : Postprint (Author's version)

References

1. J. Wan, B. Fan and S. H. Thang, Chemical Science, 2022, 13, 4192–4224.
2. H. Phan, V. Taresco, J. Penelle and B. Couturaud, Biomater. Sci., 2021, 9, 38–50.
3. C. Liu, C.-Y. Hong and C.-Y. Pan, Polym. Chem., 2020, 11, 3673– 3689.
4. C. Grazon, P. Salas-Ambrosio, E. Ibarboure, A. Buol, E. Garanger, M. W. Grinstaff, S. Lecommandoux and C. Bonduelle, Angewandte Chemie International Edition, 2020, 59, 622.
5. D. B. Wright, M. A. Touve, L. Adamiak and N. C. Gianneschi, ACS Macro Lett., 2017, 6, 925–929.
6. S. Varlas, J. C. Foster and R. K. O'Reilly, Chem. Commun., 2019, 55, 9066–9071.
7. M. J. Derry, L. A. Fielding and S. P. Armes, Progress in Polymer Science, 2016, 52, 1–18.
8. L. Lei, N. Patil, A. Arnoux, C. Le Cœur, Y. de Rancourt de Mimérand, D. Grande, B. Le Droumaguet, X. Feng, Y. Gnanou and B. Couturaud, Macromolecules, 2024, 57, 10513–10521.
9. H. Phan, R. Cavanagh, D. Destouches, F. Vacherot, B. Brissault, V. Taresco, J. Penelle and B. Couturaud, ACS Appl. Polym. Mater., 2022, 4, 7778–7789.
10. H. Phan, R. Cavanagh, P. Jacob, D. Destouches, F. Vacherot, B. Brugnoli, S. Howdle, V. Taresco and B. Couturaud, Polymers, 2023, 15, 3070.
11. N. Audureau, F. Coumes, J.-M. Guigner, T. P. T. Nguyen, C. Ménager, F. Stoffelbach and J. Rieger, Polym. Chem., 2020, 11, 5998–6008.
12. D. Ikkene, J.-L. Six and K. Ferji, European Polymer Journal, 2023, 188, 111848.
13. J. Sun and R. N. Zuckermann, ACS Nano, 2013, 7, 4715–4732.
14. N. Gangloff, J. Ulbricht, T. Lorson, H. Schlaad and R. Luxenhofer, Chem. Rev., 2016, 116, 1753–1802.
15. K. Klinker and M. Barz, Macromolecular Rapid Communications, 2015, 36, 1943–1957.
16. A M. Clapperton, J. Babi and H. Tran, ACS Polym. Au, 2022, 2, 417–429.
17. D. Zhang, S. H. Lahasky, L. Guo, C.-U. Lee and M. Lavan, Macromolecules, 2012, 45, 5833–5841.
18. M. Hartweg, C. J. C. Edwards-Gayle, E. Radvar, D. Collis, M. Reza, M. Kaupp, J. Steinkoenig, J. Ruokolainen, R. Rambo, C. Barner- Kowollik, I. W. Hamley, H. S. Azevedo and C. R. Becer, Polym. Chem., 2018, 9, 482–489.
19. A. Ma, X. Yu, M. Liao, W. Liu, S. Xuan and Z. Zhang, Macromolecular Rapid Communications, 2023, 44, 2200301.
20. R. Kakuchi, Angewandte Chemie International Edition, 2014, 53, 46–48.
21. B. Couturaud, Z. H. Houston, G. J. Cowin, I. Prokeš, J. C. Foster, K. J. Thurecht and R. K. O'Reilly, ACS Macro Lett., 2019, 8, 1479– 1483.
22. A. K. Pearce, A. Travanut, B. Couturaud, V. Taresco, S. M. Howdle, M. R. Alexander and C. Alexander, ACS Macro Lett., 2017, 6, 781–785.
23. E. Ruijter and R. V. A. Orru, Drug Discovery Today: Technologies, 2013, 10, e15–e20.

Published in : Polymer Chemistry (2025), vol. 16, n°26, pp. 3041–3050
DOI: 10.1039/D5PY00384A
Status : Postprint (Author's version)

24. E. Ruijter, R. Scheffelaar and R. V. A. Orru, Angewandte Chemie International Edition, 2011, 50, 6234–6246.
25. O. Kreye, O. Türünç, A. Sehlinger, J. Rackwitz and M. A. R. Meier, Chemistry – A European Journal, 2012, 18, 5767–5776.
26. A. C. Boukis, A. Llevot and M. A. R. Meier, Macromolecular Rapid Communications, 2016, 37, 643–649.
27. A. C. Boukis and M. A. R. Meier, European Polymer Journal, 2018, 104, 32–38.
28. W. Konrad, F. R. Bloesser, K. S. Wetzel, A. C. Boukis, M. A. R. Meier and C. Barner-Kowollik, Chemistry – A European Journal, 2018, 24, 3413–3419.
29. P.-K. Dannecker, A. Sehlinger and M. A. R. Meier, Macromolecular Rapid Communications, 2019, 40, 1800748.
30. X. Zhang, S. Wang, J. Liu, Z. Xie, S. Luan, C. Xiao, Y. Tao and X. Wang, ACS Macro Lett., 2016, 5, 1049–1054.
31. P. Stiernet, B. Couturaud, V. Bertrand, G. Eppe, J. De Winter and A. Debuigne, Polym. Chem., 2021, 12, 2141–2151.
32. A. A. Samad, J. D. Winter, P. Gerbaux, C. Jérôme and A. Debuigne, Chem. Commun., 2017, 53, 12240–12243.
33. Y. Tao, S. Wang, X. Zhang, Z. Wang, Y. Tao and X. Wang, Biomacromolecules, 2018, 19, 936–942.
34. M. Saimura, M. Takehara, S. Mizukami, K. Kataoka and H. Hirohara, Biotechnol Lett, 2008, 30, 377–385.
35. I.-L. Shih, M.-H. Shen and Y.-T. Van, Bioresource Technology, 2006, 97, 1148–1159.
36. J.-N. Liu, S.-L. Chang, P.-W. Xu, M.-H. Tan, B. Zhao, X.-D. Wang and Q.-S. Zhao, J. Agric. Food Chem., 2020, 68, 1101–1109.
37. Y. Wang, L. Wang, Y. Hu, J. Qin and B. Yu, International Journal of Biological Macromolecules, 2024, 262, 129513.
38. A. Traeger and M. N. Leiske, Biomacromolecules, 2025, 26, 5–32.
39. M. Li and Y. Tao, Polym. Chem., 2021, 12, 1415–1424.
40. B. Yang, Y. Zhao, X. Ren, X. Zhang, C. Fu, Y. Zhang, Y. Wei and L. Tao, Polym. Chem., 2014, 6, 509–513.
41. H. Wu, B. Yang, Y. Zhao, Y. Wei, Z. Wang, X. Wang and L. Tao, Polym. Chem., 2016, 7, 4867–4872.
42. A. Yang, Y. Zhao, C. Fu, C. Zhu, Y. Zhang, S. Wang, Y. Wei and L. Tao, Polym. Chem., 2014, 5, 2704–2708.
43. X. Pan, F. Zhang, B. Choi, Y. Luo, X. Guo, A. Feng and S. H. Thang, European Polymer Journal, 2019, 115, 166–172.
44. A. Kerr, G. Moriceau, M. A. Przybyla, T. Smith and S. Perrier, Macromolecules, 2021, 54, 6649–6661.
45. L. Luppi, T. Babut, E. Petit, M. Rolland, D. Quemener, L. Soussan, M. A. Moradi and M. Semsarilar, Polym. Chem., 2019, 10, 336– 344.
46. M. Semsarilar, V. Ladmiral, A. Blanazs and S. P. Armes, Langmuir, 2013, 29, 7416–7424.
47. V. Baddam, L. Välinen, L. Kuckling and H. Tenhu, Polym. Chem., 2022, 13, 3790–3799.
48. G. N. Smith, L. L. E. Mears, S. E. Rogers and S. P. Armes, Chem. Sci., 2018, 9, 922–934.